



Cite this: DOI: 10.1039/d1gc00502b

## Nanocellulose-based mechanically stable immobilization matrix for enhanced ethylene production: a framework for photosynthetic solid-state cell factories†

 V. Rissanen,<sup>‡a</sup> S. Vajravel,<sup>‡b</sup> S. Kosourov,<sup>b</sup> S. Arola,<sup>a</sup> E. Kontturi,<sup>id c</sup>  
 Y. Allahverdiyeva<sup>id \*b</sup> and T. Tammelin<sup>id \*a</sup>

Cell immobilization is a promising approach to create efficient photosynthetic cell factories for sustainable chemical production. Here, we demonstrate a novel photosynthetic solid-state cell factory design for sustainable biocatalytic ethylene production. We entrapped cyanobacteria within never-dried hydrogel films of TEMPO-oxidized cellulose nanofibers (TCNF) cross-linked with polyvinyl alcohol (PVA) to create a self-standing matrix architecture. The matrix is operational in the challenging submerged conditions and outperforms existing alginate-based solutions in terms of wet strength, long-term cell fitness, and stability. Based on rheological investigations, the critical strength of wet TCNF matrices is three times higher than in the existing immobilization matrices of alginate cross-linked with Ca<sup>2+</sup>. This is due to the rigid nature of the colloidal nanofiber network and the strong cross-linking with PVA, as opposed to polymeric alginate with reversible ionic Ca<sup>2+</sup> bonds. The porous and hygroscopic nanofiber network also shields the cyanobacterial cells from environmental stress, maintaining photosynthetic activity during partial drying of films, and when submerged in the nutrient medium for long-term cultivation. Finally, TCNF matrices allow the ethylene-producing *Synechocystis* sp. PCC 6803 cells to operate in submerged conditions under high inorganic carbon loads (200 mM NaHCO<sub>3</sub>), where Ca<sup>2+</sup>-alginate matrices fail. The latter show severe cell leakage due to matrix disintegration already within 20 min of NaHCO<sub>3</sub> supplementation. In contrast, TCNF-based matrices prevent cell leakage to the medium and restrict culture growth, leading to improved ethylene production yields. Furthermore, the operational capacity of the self-standing TCNF cell factory can be maintained long-term by periodically refreshing the nutrient medium. All in all, the results showcase the versatility and potential of cell immobilization with the never-dried colloidal TCNF matrix, paving the way towards novel biotechnological pathways using solid-state cell factories designed for efficient and sustainable production of e.g., monomers and fuels.

Received 8th February 2021.

Accepted 19th April 2021

DOI: 10.1039/d1gc00502b

[rsc.li/greenchem](http://rsc.li/greenchem)

## Introduction

Photosynthetic cell factories (PCFs) are versatile platforms promoting a circular bioeconomy, where photosynthetically active microbial cells of cyanobacteria and green algae are used as biocatalysts for sustainable production of targeted biochemi-

cals and biofuels. These photosynthetic microbes use solar energy, water and trace mineral nutrients to create chemical energy by splitting water to O<sub>2</sub> and assimilating atmospheric CO<sub>2</sub> into biomass and energy-rich organic compounds from monomers to complex bioactive compounds.<sup>1,2</sup> One such compound is ethylene, a major chemical building block and an attractive fuel source that is currently produced from fossil sources using energy-intensive steam-cracking, which generates significant amounts of greenhouse gases and toxic co-products.<sup>3,4</sup>

To improve the production efficiency of traditional PCFs based on suspension culturing, many of its physiological and technical drawbacks can be overcome by immobilizing the photosynthetic cells, *i.e.* distributed within a thin layer of the solid or gel-like carrier matrix.<sup>5–8</sup> This transition can improve light-to-product conversion efficiency by enabling more

<sup>a</sup>VTT Technical Research Centre of Finland Ltd, VTT, PO Box 1000, FI-02044 Espoo, Finland. E-mail: [tekla.tammelin@vtt](mailto:tekla.tammelin@vtt)
<sup>b</sup>Molecular Plant Biology, Department of Life Technologies, University of Turku, Turku, FI-20014, Finland. E-mail: [allahve@utu.fi](mailto:allahve@utu.fi)
<sup>c</sup>Department of Bioproducts and Biosystems, Aalto University, Espoo FI-00076, Finland

†Electronic supplementary information (ESI) available. See DOI: 10.1039/d1gc00502b

‡These authors contributed equally.



uniform irradiation of photosynthetic cells and restricting cell division, while simultaneously reducing water and energy consumption.<sup>9,10</sup> Cell immobilization has been shown to increase the yield of ethylene production by 2-fold when compared to suspended cells, as well as the light-to-ethylene conversion efficiency by 3.5 times<sup>4</sup> under non-submerged conditions. Using alginate cross-linked with divalent cations (*e.g.* Ca<sup>2+</sup> and Ba<sup>2+</sup>) has been the conventional state-of-the-art solution for immobilizing green algae and cyanobacteria, despite its limitations in mechanical properties, such as wet strength and porosity.<sup>11–13</sup> Alginate-based matrices are especially poorly suited for many environments with high ionic concentrations, such as wastewaters,<sup>6,14</sup> as their ionic bonds are reversible depending on the concentration and species of the surrounding ions.<sup>6,15</sup> Similarly, biocatalytic ethylene production with cyanobacteria presents especially challenging conditions, as Vajravel *et al.* (2020) reported that the optimal production requires the addition of 200 mM sodium bicarbonate (NaHCO<sub>3</sub>) as an inorganic carbon supplement, which leads to precipitation of Ca<sup>2+</sup> ions as insoluble CaCO<sub>3</sub>, disrupting the Ca-cross-linking of alginate. Thus, a liquid-conveying intermediate was used to support the alginate matrix.<sup>4</sup>

Here, we present a novel solid-state cell factory matrix design exemplified by efficient biocatalytic ethylene production with entrapped cyanobacteria. The self-standing matrix architecture, which utilises never-dried hydrogel thin films from TEMPO-oxidized cellulose nanofibers (TCNF),<sup>16</sup> is able to operate in challenging conditions of submerged cultivation. The synergistic advantages of this design are two-fold: firstly, it provides direct transportation of water, nutrient, gases and light for the cells. Secondly, the high mechanical stability of the nanoscale fibril network enables the cell factory to operate without any supporting structures, thus outperforming the proof-of-concept matrices we have presented earlier.<sup>13</sup> The immobilization framework architecture is achieved by cross-linking the never-dried TCNF hydrogel with both chemical and ionic means using polyvinyl alcohol (PVA)<sup>17</sup> and Ca<sup>2+</sup>,<sup>18</sup> respectively. To evidence the improved mechanical performance, we employ thorough rheological investigations to reveal the viscoelastic behaviour of the wet hydrogel matrices. Previously, wet strength measurements have been only reported for dried and rewetted TCNF-PVA films,<sup>17</sup> with several times higher values than for similar Ca<sup>2+</sup>-alginate films.<sup>15,19</sup> Furthermore, we observe that submerged TCNF-based matrices remain stable during long-term ethylene production with the NaHCO<sub>3</sub> supplemented conditions that lead to the disintegration of Ca<sup>2+</sup>-cross-linked alginate matrices.

In this paper, we showcase a novel solid-state cell factory matrix design based on never-dried colloidal TCNF network, surpassing the existing polymeric alternatives with respect to wet strength, long-term cell fitness and ethylene production yield. Nanocellulose-based matrix displays superior mechanical stability over conventionally utilised alginate systems. TCNF network fully prevented the cell leakage and matrix disintegration in challenging ethylene photoproduction conditions. These discoveries have the potential to revolutionize

the cell factory concept by providing pathways to overcome the bottlenecks related to excessive water consumption, low volumetric productivity and inefficient light utilization.

## Experimental

### Materials

**Cyanobacterial strains and growth conditions.** The wild-type *Synechocystis* sp. strain PCC 6803 (hereby “WT cells”) and the *efe* mutant S5 of *Synechocystis* sp. PCC 6803 (hereby “mutant cells”) were used in this study. The *efe* mutant S5 was generated by heterologous expression of ethylene forming enzyme (Efe) from *Pseudomonas syringae* as described by Thiel *et al.*<sup>20</sup> The cyanobacterial cultures were maintained on a BG11 medium<sup>21</sup> buffered with 20 mM HEPES–NaOH (pH 7.5) under agitation using a rotary shaker (120 rpm). The cultures were continuously illuminated with fluorescent lamps (Philips TL-D 36 W/865) providing 35 μmol photons per m<sup>2</sup> per s PAR (Photosynthetically Active Radiation) at 30 °C in the growth chamber supplied with 1% CO<sub>2</sub>. The stock cultures of the *efe* mutant were supplemented with 10 μg mL<sup>-1</sup> chloramphenicol and 25 μg mL<sup>-1</sup> spectinomycin. Experimental cultures of both strains were grown in 1 L Roux bottles containing 600 mL of BG11 medium (pH 7.5) without antibiotics. The cultures were routinely sparged with sterile air (filtered through a 0.2 μm pore-size filter, Acro 37 TF, Gelman Sciences, USA) supplemented with 1% CO<sub>2</sub>. For all experiments, cells were harvested by centrifugation (at 5000 g for 5 min) at their exponential growth phase (~ 0.8–1.0 OD<sub>750</sub>).

**TEMPO-oxidized cellulose nanofibers (TCNF).** Cellulose nanofibers were produced from never-dried bleached softwood pulp (a mixture of spruce and pine) obtained from a Finnish pulp mill. TEMPO-mediated oxidation of the pulp fibres was performed by alkaline hypochlorite oxidation catalysed by TEMPO, according to the protocol described by Saito *et al.*<sup>16</sup> The anionic charge of the oxidized pulp, determined with a standard conductometric titration method (SCAN 65:02), was 1.45–1.52 mmol g<sup>-1</sup>. After TEMPO-oxidation the pulp was washed and fibrillated into CNF (hereby TCNF) in a microfluidizer (Microfluidics Int., USA) equipped with two Z-type chambers with diameters of 400 and 100 μm, respectively. The pulp was fibrillated for two passes at 1850 bar operating pressure, with final consistency of TCNF *ca.* 1 wt%. The appearance of TCNF is that of a viscous and transparent hydrogel. The carbohydrate composition of TCNF is 64.0% glucose, 6.2% xylose and 2.1% mannose.<sup>22</sup>

**Polymers.** 2 wt% alginate solution used for reference matrices was prepared by mixing Na-alginate salt from brown algae (#71238, Sigma-Aldrich) in Milli-Q water. Polyvinyl alcohol (Mowiol 56–98, *M*<sub>w</sub> 195 000 g mol<sup>-1</sup>, DP 4300) used as a cross-linking additive to improve the wet strength of TCNF gels was purchased from Sigma-Aldrich and dissolved to a 5 wt% solution in Milli-Q water at 95 °C.

**Other chemicals and materials.** All chemicals were of analytical grade and used as received. 2,2,6,6-



Tetramethylpiperidin-1-oxyl (TEMPO), sodium bromide (solid) and 10% sodium hypochlorite (aqueous) were purchased from Sigma-Aldrich. 0.1 M sodium hydroxide solution was obtained from Fluka Analytical.  $\text{CaCl}_2$  (99%, #C7902) was purchased from Sigma-Aldrich. Ultrapure water (18.2 M $\Omega$  cm) was prepared with a Milli-Q purification unit (QPAK® 1, Millipore). A commercial Teflon (PTFE) film (Etra, Finland) was used as a scaffold during the preparation of PVA-cross-linked  $\text{Ca}^{2+}$ -TCNF and  $\text{Ca}^{2+}$ -alginate hydrogel films.

## Methods

**Immobilization procedures.** Cyanobacterial cells were immobilized according to the concept shown in Fig. 1. To accommodate for the different measurement setups, three Experimental Designs with slight variations, labelled as Designs #1, #2 and #3, were prepared as explained below. Table 1 summarizes the properties of the Experimental Designs.

**Experimental design #1.** Design #1 includes the preparation of self-standing PVA-cross-linked  $\text{Ca}^{2+}$ -TCNF hydrogel films (Fig. 2A, hereby PVA- $\text{Ca}^{2+}$ -TCNF) and  $\text{Ca}^{2+}$ -cross-linked alginate hydrogel films (Fig. 2B, hereby  $\text{Ca}^{2+}$ -alginate), which were used for determining the wet strength of the immobilization

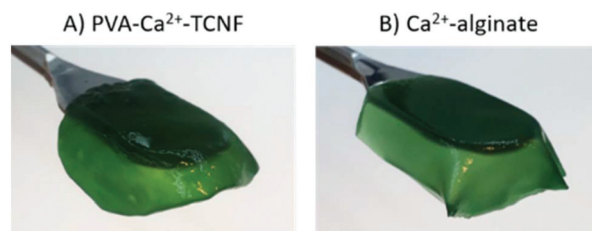


Fig. 2 Visual appearance of the never-dried hydrogel films containing immobilized cyanobacterial cells. (A) Self-standing PVA- $\text{Ca}^{2+}$ -TCNF, and (B)  $\text{Ca}^{2+}$ -alginate.

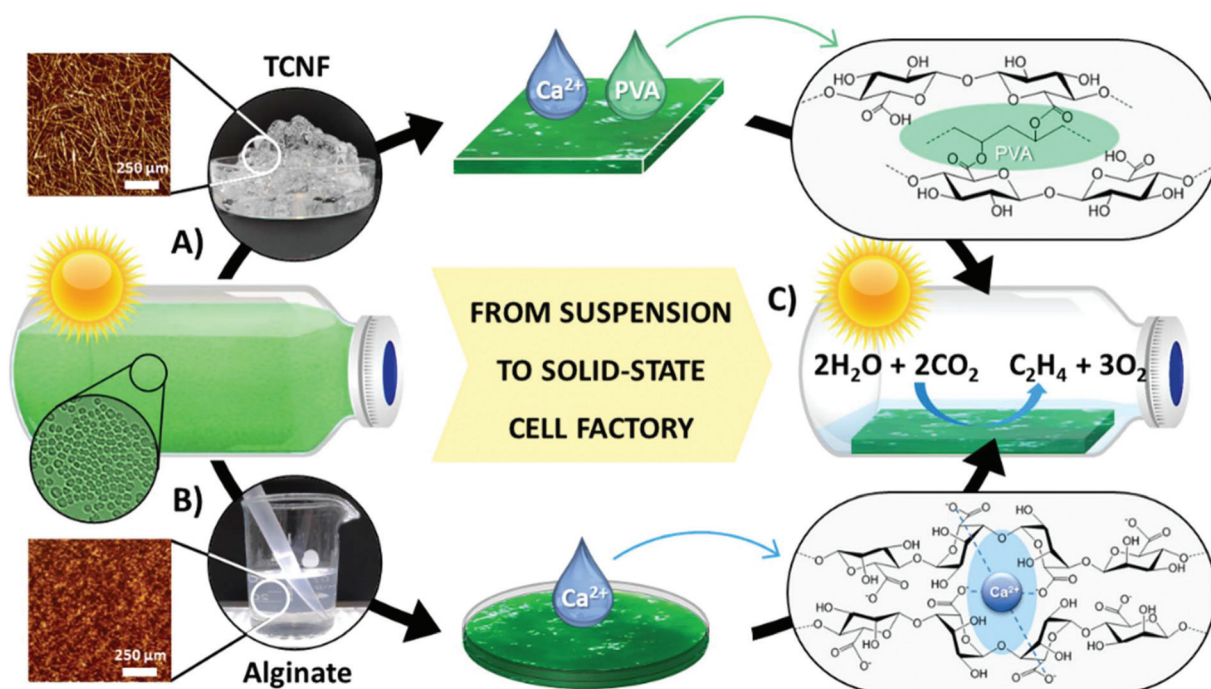


Fig. 1 Concept for solid-state cell factories. The schematic representation of the experimental approach for immobilizing ethylene-producing mutant cells within TCNF- and alginate-based matrices. The appearance, AFM phase topography images, cross-linking mechanism and chemical structure of (A) colloidal TCNF network cross-linked with polyvinyl alcohol (PVA), and (B) dissolved alginate polymer chains with  $\text{Ca}^{2+}$ -crosslinking are shown. (C) A representation of solid-state cell factory with the chemical formula for photosynthetic ethylene production by the immobilized mutant cells. The Z ranges for AFM images are 10 nm for TCNF and 2 nm for alginate, respectively.

Table 1 Summary of matrix design parameters

	Wet matrix	Cross-link	Water removed	Sample handling
Experimental design #1	1% TCNF 2% Alginate	$\text{Ca}^{2+}$ , PVA $\text{Ca}^{2+}$	50% 0%	Cut in circles ( $d = 5$ cm)
Experimental design #2	1% TCNF 1% Alginate	$\text{Ca}^{2+}$ , PVA $\text{Ca}^{2+}$	10–100% 10–100%	Cut in $\sim 5 \times 5$ cm pieces
Experimental design #3	1% TCNF 1% Alginate	$\text{Ca}^{2+}$ , PVA $\text{Ca}^{2+}$	50% 50%	Cut in $3 \times 1$ cm strips



matrices in rheology measurements. Technical triplicates of all samples were prepared for the measurements. For the preparation of PVA-Ca<sup>2+</sup>-TCNF, WT cells in a suspension of BG11 medium were entrapped within a hydrogel consisting of 1 wt% TCNF and 0.1 wt% PVA. Before mixing, the cells were concentrated to the optical density of ~1.0 at 720 nm (OD<sub>720</sub>) by centrifuging at 5000 g for 5 minutes, removing the supernatant and resuspending the cells to fresh BG11 medium. Equal amounts of cell suspension and hydrogel were mixed using a T 25 digital Ultra-Turrax homogenizer (IKA, Staufen, Germany) at 12 000 rpm for 1 minute. Air bubbles were removed *via* centrifugation at 3000g for 5 minutes, and the hydrogels were spread onto a Teflon film using a handheld coating applicator with a 2 mm gap at high speed to achieve sufficient shear forces for even spreading. Cross-linking with PVA was induced by evaporating water in a controlled temperature of 23 °C and relative humidity (RH) of 50%, until 50 wt% of water was evaporated from the samples, resulting in a final TCNF concentration of 1 wt%. Gelation of TCNF with calcium ions was induced by spraying of 50 mM CaCl<sub>2</sub> onto the samples until they were fully wetted and waiting for 15 minutes before dipping the samples in a bath of 50 mM CaCl<sub>2</sub> for additional 15 minutes to ensure full gelation. The hydrogel films were cut into circular pieces (*d* = 5 cm) and allowed to swell in a Petri dish filled with BG11 medium at low light for 24 hours prior to measurements. Control samples with BG11 medium without cells were prepared in the same way.

For preparation of Ca<sup>2+</sup>-alginate assemblies, WT cells in a suspension of BG11 medium were entrapped within alginate hydrogel similarly to preparation of Ca<sup>2+</sup>-TCNF-PVA, except 2 wt% alginate was used and no PVA was added. The formulation of cells and alginate was spread onto a Teflon film using a pipette until a thickness of 1 mm was achieved. The water evaporation used for PVA-Ca<sup>2+</sup>-TCNF was not applied, resulting in a final concentration of 1 wt%. Control samples with BG11 medium without cells were prepared in the same way.

**Experimental design #2.** Design #2 was used to assess the recovery and long-term fitness of immobilized WT cells. Biological duplicates of each sample were prepared. PVA-Ca<sup>2+</sup>-TCNF and Ca<sup>2+</sup>-alginate hydrogel films with immobilized WT cells were prepared as described in Design #1, except 1 wt% alginate was used, and water evaporation was applied to both materials. Ten different samples were prepared for each material, where 10–100% of the total water content was evaporated at 10% intervals between the samples. The Ca<sup>2+</sup>-gelation was performed prior to the evaporation by spraying 50 mM CaCl<sub>2</sub> onto the samples until they were completely wetted and waiting for 30 minutes. The samples were rinsed with MilliQ water, cut into ~5 × 5 cm pieces, placed in Petri dishes (20 cm diameter) filled with 40 ml of BG11 medium, and kept at low light for photosynthetic activity monitoring.

**Experimental design #3.** Design #3 was used for estimation of ethylene production by immobilized mutant cells. The cells were entrapped within PVA-Ca<sup>2+</sup>-TCNF and Ca<sup>2+</sup>-alginate as described in Design #1 with the following exceptions: 1 wt%

alginate was used and water evaporation was applied as described for PVA-Ca<sup>2+</sup>-TCNF until 50% of the water is evaporated from the samples, resulting in 1 wt% concentration. After the Ca<sup>2+</sup>-cross-linking, the samples were cut into 3 × 1 cm strips and used immediately in the ethylene production assay.

**Ethylene production assay and ethylene quantification.** The ethylene-producing mutant cells entrapped within PVA-Ca<sup>2+</sup>-TCNF and Ca<sup>2+</sup>-alginate as described in Experimental Design #3 were submerged into 3 mL of BG11 medium in 23.5 mL gas-tight vials sealed with Teflon-coated rubber stoppers. The medium was supplemented with 200 mM NaHCO<sub>3</sub> (1 M NaHCO<sub>3</sub> stock solution freshly prepared in BG11 medium) as the inorganic carbon (Ci) source<sup>4</sup> and 1 mM IPTG (isopropyl-β-D-thiogalactopyranoside, 100 mM stock), functioning as an inducer. IPTG is a sugar derivative used for the induction of the recombinant protein expression in *Synechocystis* sp. PCC 6803, which is controlled by the Lac promoter.<sup>20</sup> The vials were incubated in a growth chamber under continuous illumination of 35 μmol photons per m<sup>2</sup> per s PAR supplied with fluorescence lamps (Philips TL-D 36 W/865) at 30 °C. The amount of ethylene was monitored every 24 h by using a gas chromatograph (GC, Clarus 580, PerkinElmer, Inc.). The instrument was equipped with a capillary column (Carboxen 1010 PLOT 30 m × 0.53 mm) and a flame ionization detector set at 150 °C with H<sub>2</sub> and air flows fixed at 30 mL min<sup>-1</sup> and 300 mL min<sup>-1</sup>, respectively. Argon (AGA, Finland) was used as a carrier gas at a flow rate of 9.8 mL min<sup>-1</sup> (18 psi). A 40 μl gas sample was collected from the headspace of the vials using a gas-tight Hamilton syringe (Hamilton Company, USA), and injected into the GC instrument. For the quantification of ethylene, the calibration curve was obtained using different volumes of a commercial gas standard (1% v/v C<sub>2</sub>H<sub>4</sub> in N<sub>2</sub>, AGA, Finland). The yield of ethylene was normalized to the initial total chlorophyll *a* (Chl *a*) content of the films.

**Photosynthetic activity.** The effective yield of photosystem II (Y(II)) of WT and mutant cells was measured using AquaPen-C AP-C 100 hand-held fluorometer (Photon Systems Instruments, Czech Republic). Before measurements, the sample was placed into the cuvette of the AquaPen-C AP-C 100. Y(II) in a light-adapted state was obtained by applying a strong light pulse (3000 μmol m<sup>-2</sup> s<sup>-1</sup>, 600 ms) on the actinic light (50 μmol m<sup>-2</sup> s<sup>-1</sup>) background.

**Chl *a* determination.** The entrapped cells in PVA-Ca<sup>2+</sup>-TCNF and Ca<sup>2+</sup>-alginate were incubated with 90% methanol at 65 °C for 30 min under dark conditions after which the supernatant was used for the measurements. The Chl content was determined spectrophotometrically at 665 nm with an extinction coefficient of 12.7 mg L<sup>-1</sup> cm A<sup>-1</sup>.<sup>23</sup>

**Rheological measurements.** Rheological measurements were performed using a Discovery HR-2 – Rheometer (TA Instruments, New Castle, Delaware, USA) at 22 °C with a serrated plate–plate geometry (diameter 40 mm) to avoid slip. The viscoelastic properties of PVA-Ca<sup>2+</sup>-TCNF and Ca<sup>2+</sup>-alginate hydrogel films, prepared as described in Experimental Design #1, were investigated *via* small deformation oscillatory stress and frequency sweep tests. In these experiments, storage



modulus ( $G'$ ) represents the elastic component and loss modulus ( $G''$ ) the viscous component of the sample. The loss tangent or damping factor ( $\tan \delta$ ) represents the ratio of loss to storage modulus ( $G''/G'$ ), and critical stress signifies the onset at which irreversible plastic deformation occurs. The stress sweep tests were performed between 0.05 and 200 Pa under a constant frequency of 0.1 Hz, and the frequency sweep tests (between 0.05 and 100 Hz at a constant stress of 0.1 Pa. All samples were allowed to relax for 2 min under the measuring head prior to measurements.

## Results and discussion

### Wet strength of immobilization matrices with rheology measurements

Small deformation oscillatory stress sweeps and frequency sweeps (ESI<sup>†</sup>) were performed on PVA-Ca<sup>2+</sup>-TCNF and Ca<sup>2+</sup>-alginate hydrogel films prepared as described for Experimental Design #1, both with and without WT cells. The elastic modulus ( $G'$ ), viscous modulus ( $G''$ ) and  $\tan \delta$  values ( $G''$  divided by  $G'$ ) of typical stress sweep measurement for each sample are presented in Fig. 3. As the figure shows, the

average  $G'$  values in the linear viscoelastic region for both PVA-Ca<sup>2+</sup>-TCNF and Ca<sup>2+</sup>-alginate samples are approximately an order of magnitude higher than  $G''$ , indicating the systems are predominantly elastic (solid-like). However, they reach a crossover point where  $G''$  surpasses  $G'$  after the onset of non-linear behaviour at critical stress, or yield stress, where the system becomes predominantly viscous. Similarly, frequency sweep measurements (Fig. S1<sup>†</sup>) show a linear behaviour for all samples under time-dependent stress until the crossover point at around 50 Hz. After this, the system is no longer able to reliably measure the samples and the values begin to change beyond the sensitivity limits of the device. For all samples, the cross-over is seen at similar frequencies, indicating that all gels are similarly stable under oscillatory frequency, and unaffected by time-dependent small deformation stress.

Fig. 4A shows a comparison of the  $\tan \delta$  values between typical stress sweeps of PVA-Ca<sup>2+</sup>-TCNF and Ca<sup>2+</sup>-alginate hydrogel films with and without WT cells. In the linear region, the  $\tan \delta$  values are  $\sim 0.07$  Pa for PVA-Ca<sup>2+</sup>-TCNF and  $\sim 0.12$  Pa for Ca<sup>2+</sup>-alginate. Moreover, critical stress occurs significantly later for PVA-Ca<sup>2+</sup>-TCNF than for Ca<sup>2+</sup>-alginate. As shown in Fig. 4B, the average  $G'$  and  $G''$  values in the linear viscoelastic region for PVA-Ca<sup>2+</sup>-TCNF with WT cells are  $\sim 1000$  Pa and  $\sim 75$  Pa, respectively, and the average critical stress is  $\sim 70$  Pa. For the same system without cells,  $G'$  increases to  $\sim 1300$  Pa while  $G''$  remains relatively unchanged, and critical stress increases to  $\sim 75$  Pa. For Ca<sup>2+</sup>-alginate with WT cells, the  $G'$  and  $G''$  values are  $\sim 1200$  Pa and 160 Pa, respectively, and critical stress is around 20 Pa. Without cells,  $G'$  and  $G''$  are significantly higher, with values of 1600–2200 Pa, and  $\sim 220$  Pa, respectively. Similarly, the critical stress increases to  $\sim 40$  Pa.

Mechanical wet-strength testing of cross-linked TCNF and alginate gels and films is often carried out *via* either large-deformation tensile strength tests,<sup>17,24,25</sup> rheological measurements,<sup>26,27</sup> or a combination of both.<sup>28–30</sup> However, tensile tests are predominantly performed with once-dried films, and therefore do not suit the never-dried hydrogel films demonstrated here. Nonetheless, there is literature for wet tensile strength measurements using TCNF-PVA and Ca<sup>2+</sup>-alginate in different conditions. Hakalahti *et al.*<sup>17</sup> reported tensile strength of approximately 30 MPa for dried TCNF-PVA -films that had been immersed in water for 24 hours, whereas Sikareepaisan *et al.*<sup>15</sup> and Pereira *et al.*<sup>19</sup> reported values ranging from 3 to 9 MPa for Ca<sup>2+</sup>-alginate films immersed in water for 30 seconds before the measurement. Here, we use small-deformation rheological measurements to reveal the viscoelastic materials properties and internal interactions of self-standing never-dried PVA-Ca<sup>2+</sup>-TCNF and Ca<sup>2+</sup>-alginate hydrogel films in the wet state.

The relatively similar  $G'$ ,  $G''$  and critical stress values of PVA-Ca<sup>2+</sup>-TCNF with and without WT cells (Fig. 3 and 4B) demonstrate that their viscoelastic properties are mostly independent of the cells, at least within the time scale of this experiment ( $\sim 24$  hours). These results indicate that the cells are not strongly interacting with TCNF but passively entrapped within the fibrillar network matrix. Moreover, the percolation

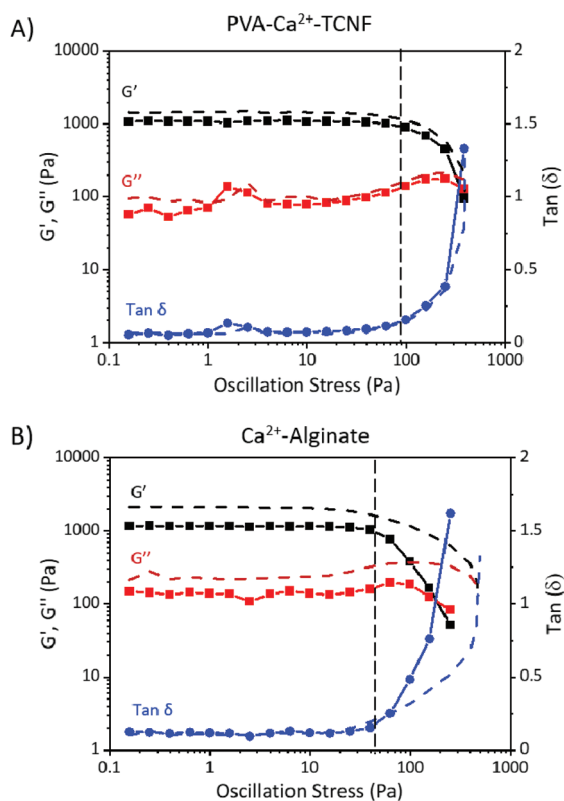


**Fig. 3** Small deformation oscillatory rheology of matrix hydrogel films. Typical stress sweeps of (A) PVA-Ca<sup>2+</sup>-TCNF and (B) Ca<sup>2+</sup>-alginate hydrogel films with (solid lines) and without (dotted lines) *Synechocystis* sp. PCC6803 wild-type (WT) cells, showing elastic moduli ( $G'$ , black square), viscous moduli ( $G''$ , red square) and  $\tan \delta$  (blue circle). The dashed vertical line marks the onset of critical stress, where the material begins to flow.



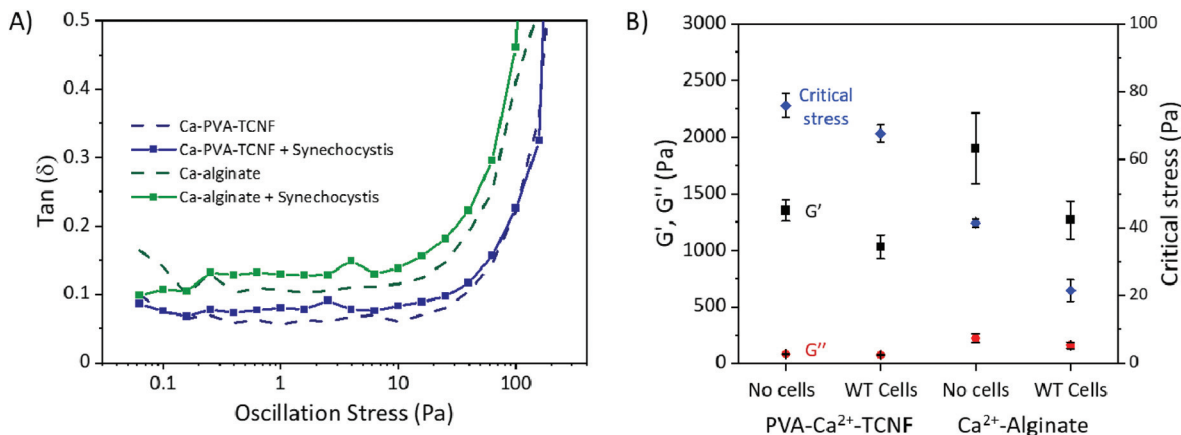


**Fig. 4** Comparison of rheological properties of *Synechocystis* sp. PCC6803 s wild-type (WT) cells immobilized within PVA-Ca<sup>2+</sup>-TCNF and Ca<sup>2+</sup>-alginate hydrogel films. (A) Tan  $\delta$  values during stress sweep. (B) Average values for elastic moduli ( $G'$ , black square), viscous moduli ( $G''$ , red circle) and the critical stress (blue diamond) values of PVA-Ca<sup>2+</sup>-TCNF and Ca<sup>2+</sup>-alginate hydrogel films with and without the cells.

of the rigid network is not largely affected by the presence of the cells. Conversely, the larger difference in these values in Ca<sup>2+</sup>-alginate with and without the cells suggests that the inclusion of cells influences significantly the interactions of the alginate polymer matrix. The cells might also disrupt the Ca<sup>2+</sup>-bonding between alginate polymer chains by bonding competitively with the Ca<sup>2+</sup>-ions. Moreover, the larger variance in rheology results for Ca<sup>2+</sup>-alginate compared to PVA-Ca<sup>2+</sup>-TCNF is potentially caused by the less specific nature of the ionic Ca<sup>2+</sup> bonding between carboxylates in alginate compared to the bridging between the hydroxyl/carboxyl groups of TCNF and PVA chains. Similarly, the higher elastic moduli of Ca<sup>2+</sup>-alginate hydrogels compared to PVA-Ca<sup>2+</sup>-TCNF may be due to interactions between Ca<sup>2+</sup>-alginate and the cells. However, as Fig. 4A shows, the tan  $\delta$  values of Ca<sup>2+</sup>-alginate are higher compared to PVA-Ca<sup>2+</sup>-TCNF, indicating they are more viscous (liquid-like) of the two systems. Similarly, TCNF-based samples have significantly higher critical stress than Ca<sup>2+</sup>-alginate, and thus they tolerate a higher shear stress before the structure yields. These results are likely due to the more rigid structure of colloidal nanocellulose fibril network compared to more flexible polymeric alginate, and the higher strength of the cross-links between TCNF and PVA chains compared to the ionic bonds between alginate polymer chains and Ca<sup>2+</sup>.

As described by Hakalahti *et al.*,<sup>17,31</sup> the wet strength of dried and rewetted TCNF films cross-linked with PVA is due to covalent cross-linking occurring between the carboxyl groups present in TCNF, and the hydroxyl groups of PVA *via* an esterification reaction. Our results suggest indirectly that the partial removal of water in the PVA-Ca<sup>2+</sup>-TCNF hydrogel films can induce a similar reaction to some degree, and a direct verification warrants further investigations.

#### Effect of matrix material and water content on long-term fitness of immobilized cells

To create water-stable PVA-Ca<sup>2+</sup>-TCNF and Ca<sup>2+</sup>-alginate hydrogel films, samples with immobilized WT cells were prepared

by mixing and controlled evaporation of water (drying) as described in Experimental Design #2. Ten different samples were prepared for both materials, where 0–90% of the total water content was gradually reduced by evaporation at 10% intervals. The samples were placed into Petri dishes filled with 40 ml of BG-11 medium, and their photosynthetic activity ( $Y_{(II)}$ ) was monitored regularly for 9 weeks. Furthermore, a visual assessment was used to estimate the mechanical stability of the submerged hydrogel films.

The photosynthetic activity ( $Y_{(II)}$ ) and the visual appearance of the hydrogel films with immobilized WT cells are presented in Fig. 5. As shown in the highlighted area of the figure, the  $Y_{(II)}$  of the cells in all samples decreases after the evaporation of water, which indicates that the drying causes stress to the cells. The  $Y_{(II)}$  values also decrease more for the Ca<sup>2+</sup>-alginate, except for samples with 20–30% water (Fig. 5D). However, the  $Y_{(II)}$  values begin to quickly increase afterwards as the cells recover, reaching similar values as before the immobilization. Samples with 30–20% water had some unrecovered areas near the edges of the hydrogel films, but samples with 10–0% water did not recover from the drying ( $Y_{(II)} = 0$ , Fig. S2<sup>†</sup>) and are excluded from the remaining discussion of the results. After 9 weeks, the photosynthetic activity remained higher for the cells entrapped within PVA-Ca<sup>2+</sup>-TCNF ( $Y_{(II)} \sim 0.37$ ) than within Ca<sup>2+</sup>-alginate ( $Y_{(II)} \sim 0.31$ – $0.35$ ), suggesting that the polymeric alginate network does not protect the cells from environmental stress as well as the colloidal TCNF network.

Based on the visual appearance, PVA-Ca<sup>2+</sup>-TCNF hydrogel films with 70–20% water remained stable in submerged conditions throughout the experiment, with no remarkable differences in stability between them. In contrast, the PVA-Ca<sup>2+</sup>-TCNF with 80–90% remaining water appeared less stable in submerged conditions, with small pieces detaching from the gels (Fig. S3<sup>†</sup>). These results suggest that ~30–60% of water should be removed to form a cross-link strong enough between TCNF and PVA and to improve the mechanical stability of the hydrogel films for cultivation in submerged con-



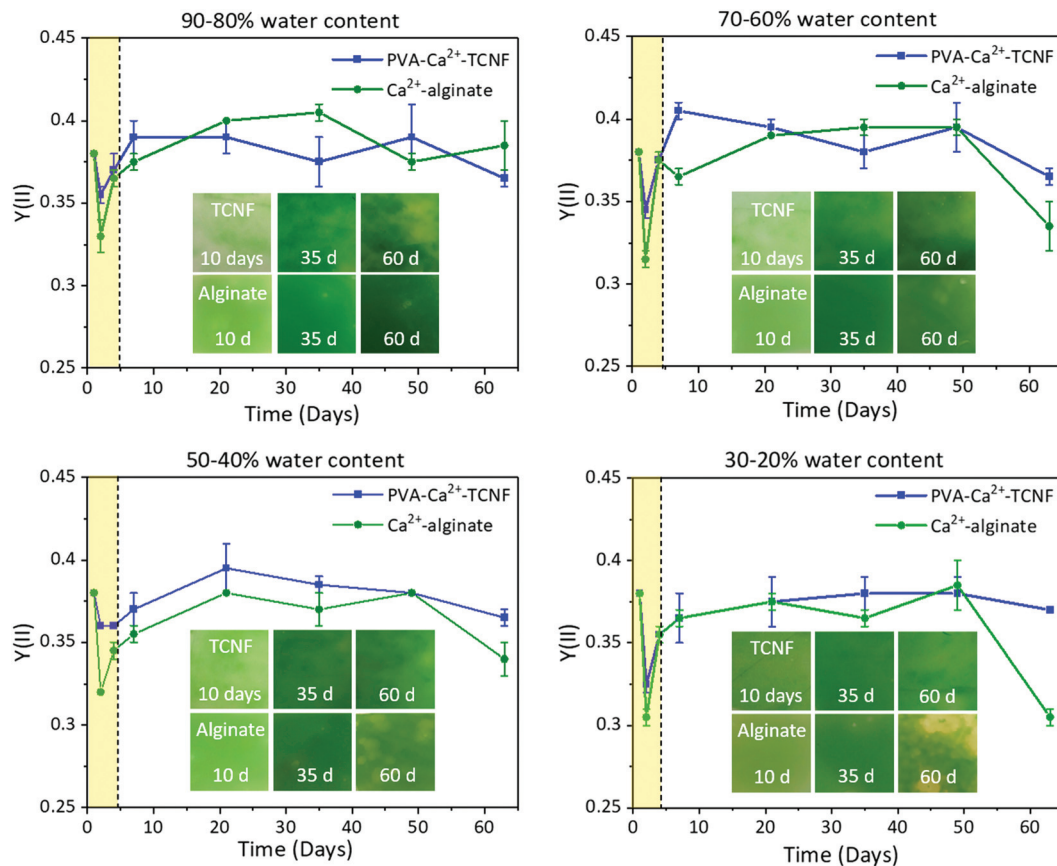


**Fig. 5** The long-term performance of *Synechocystis* sp. PCC6803 wild-type (WT) cells immobilized within PVA-Ca<sup>2+</sup>-TCNF and Ca<sup>2+</sup>-alginate. The samples were dried to 20–90% of original water content, at 10% intervals. Photosynthetic activity Y(II) and photographs are shown as a function of incubation time in a Petri dish filled with 40 ml of BG11 medium. The area highlighted with yellow colour and dotted line denote the period of drying, causing stress to the cells shown as a drop in Y(II), and the subsequent recovery after rewetting.

ditions without causing the irreversible stress to cells. We have previously demonstrated a different method to prepare PVA-crosslinked TCNF films with immobilized cyanobacteria *via* drying the formulation at 70% RH for 22 hours, resulting in a structure that is stable on a water conveying support but not in submerged conditions.<sup>13</sup> For Ca<sup>2+</sup>-alginate, all samples appeared to remain stable in submerged conditions throughout the experiment. However, the samples with 80–90% remaining water had higher Y(II) values than the ones with less water during the experiment, and especially after 8 weeks. Moreover, the samples with 20–30% of remaining water began to visibly bleach after 7 weeks, as shown in the photographs in Fig. 5. This indicates that drying of the Ca<sup>2+</sup>-alginate hydrogels creates stress to the cells and brings no additional benefits to the mechanical performance.

#### Ethylene production by immobilized cyanobacterial *efe* cells

Finally, we examined the effect of different immobilization matrices on genetically engineered ethylene-producing mutant cells under submerged conditions. The cells were immobilized within PVA-Ca<sup>2+</sup>-TCNF and Ca<sup>2+</sup>-alginate matrices as described in Experimental design #3, using a high optical cell density (~2 OD<sub>750</sub>). The matrices with entrapped cells were placed in

tightly sealed vials containing BG11 medium (pH 7.5). The medium was supplemented with 200 mM NaHCO<sub>3</sub> as a Ci source. According to previous experiments by Vajravel *et al.*, where NaHCO<sub>3</sub> concentrations from 20 to 600 mM were tested, 200 mM was shown to be the optimal concentration for both the ethylene productivity and viability of the immobilized mutant cells in sealed vials.<sup>4</sup> It is also worth noting that using CO<sub>2</sub> as a replacement Ci source is unfeasible in this setup, as satisfying amount of Ci equivalent to 200 mM NaHCO<sub>3</sub> would require saturating the cultivation media with 14% CO<sub>2</sub>, causing significant medium acidification. CO<sub>2</sub> could alternatively be supplied to the system “on-demand” in accordance with its consumption by the culture. However, this system would require precise microprocessor-controlled monitoring of CO<sub>2</sub> content in the bioreactor with feed-back regulation of CO<sub>2</sub> supply, and as such is a topic for future efforts.

However, within 20 minutes of the NaHCO<sub>3</sub> addition, the submerged matrices of Ca<sup>2+</sup>-alginate were already mostly disintegrated, releasing cells into the medium, as seen in Fig. 6B and E. This is caused by the disruption of the coordination bonds between Ca<sup>2+</sup> and alginate polymer chains, as Ca<sup>2+</sup> ions are precipitated from the medium and alginate gels as insoluble CaCO<sub>3</sub>. As a result, a higher number of cells (~11 μg of



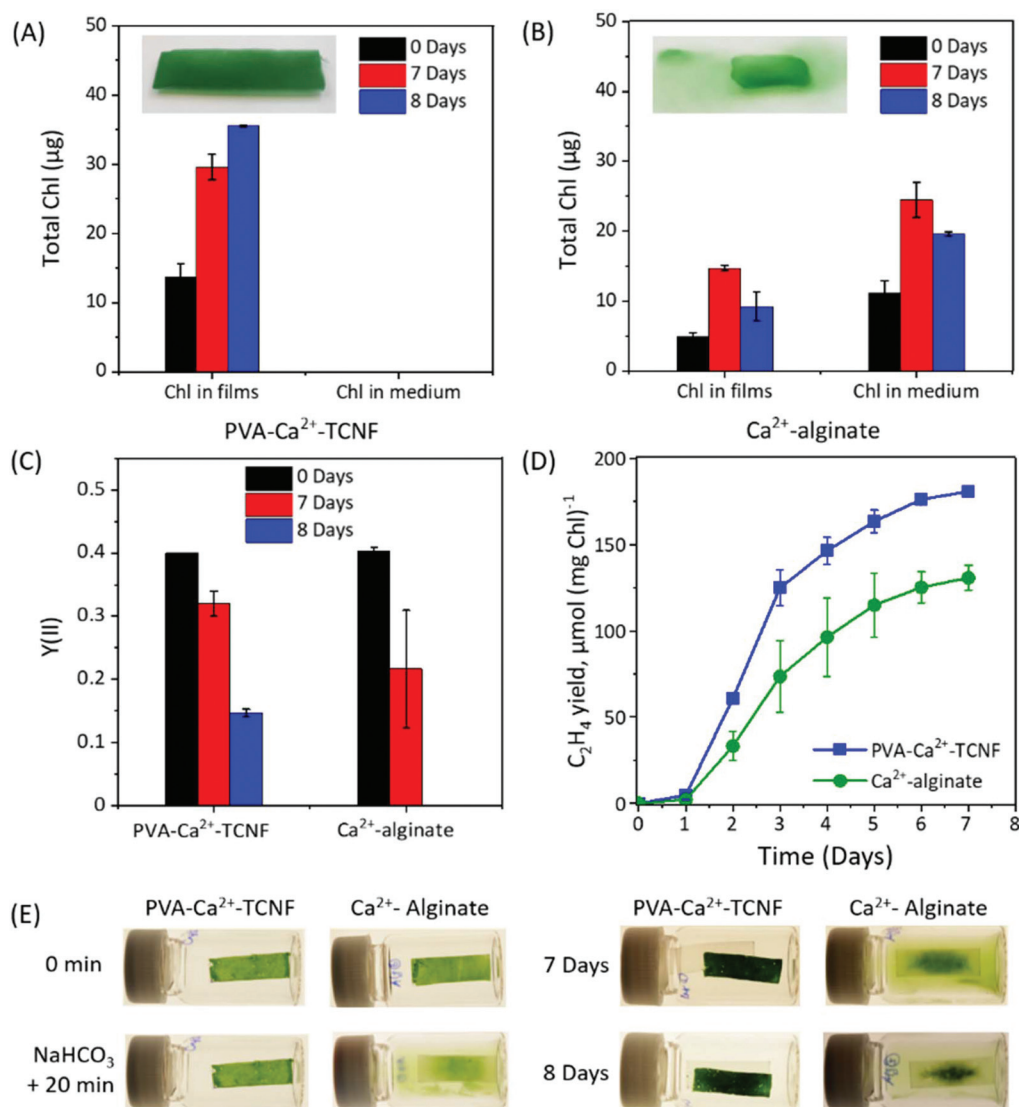


**Fig. 6** Ethylene producing capacity of the *Synechocystis* sp. PCC6803 *efe* cells entrapped within PVA-Ca<sup>2+</sup>-TCNF and Ca<sup>2+</sup>-alginate matrices under submerged production conditions. A, (B) Chl content and visual appearance of the films at 0–20 min, as well as Chl content at 7 and 8 days. (C) Photosynthetic activity. (D) Ethylene production yield calculated based on initial total Chl content. Ethylene production was initiated with an addition of IPTG (1 mM) and NaHCO<sub>3</sub> (200 mM) in sealed vials containing 3 ml of BG11 medium (pH 7.5). (E) Visual appearance of the entrapped cells in self-standing PVA-Ca<sup>2+</sup>-TCNF hydrogel film matrices, as well as in destroyed Ca<sup>2+</sup>-alginate matrices. Each experimental point represents at least 3 independent measurements from 3 vials. The error bar represents the mean of all replicates ( $\pm$ SD).

Chl) were in the medium than in the Ca<sup>2+</sup>-alginate matrix ( $\sim$ 4.8  $\mu$ g of Chl) (Fig. 6B). An additional matrix formulation with a higher (2 wt%) alginate content was also tested, resulting in similar disintegration (Fig. S4D<sup>†</sup>). In contrast, the PVA-Ca<sup>2+</sup>-TCNF matrices remained stable throughout the experiment, and no Chl was detected in the medium (Fig. 6A). Additionally, Ca<sup>2+</sup>-alginate matrices with no external support are completely disintegrated within 60 minutes in these conditions, while self-standing PVA-Ca<sup>2+</sup>-TCNF matrices remain stable and applicable (Fig. S5<sup>†</sup>). According to these results, alginate-based matrices are not suitable for chemicals production process in the submerged system with NaHCO<sub>3</sub> supplement, but TCNF-PVA-based matrices perform well under

these conditions. Notwithstanding, high photosynthetic activity ( $Y(II) = 0.4$ ) was detected for all samples (Fig. 6C). Thus, we continued with the production assay using the samples with a mixture of suspended and immobilized cells in the disintegrated Ca<sup>2+</sup>-alginate matrix (hereby referred as “destroyed Ca<sup>2+</sup>-alginate”) as a control.

As shown in Fig. 6D, all samples were able to produce ethylene for more than 7 days. The cells entrapped in PVA-Ca<sup>2+</sup>-TCNF produced  $\sim$ 180  $\mu$ mol of C<sub>2</sub>H<sub>4</sub> (mg Chl)<sup>-1</sup>, whereas the cells in Ca<sup>2+</sup>-alginate produced only  $\sim$ 130  $\mu$ mol C<sub>2</sub>H<sub>4</sub> (mg Chl)<sup>-1</sup>. After 7 days of cultivation, the photosynthetic activity ( $Y(II)$ ) of cells in the PVA-Ca<sup>2+</sup>-TCNF was  $\sim$ 0.32, whereas the photosynthetic activity of cells in destroyed Ca<sup>2+</sup>-alginate was



~0.2. The CO<sub>2</sub> uptake of the cells entrapped in PVA-Ca<sup>2+</sup>-TCNF was also 1.4-times higher compared to the cells in destroyed Ca<sup>2+</sup>-alginate (Fig. S4A†). These results indicate that cell immobilization within the PVA-Ca<sup>2+</sup>-TCNF matrix improves their photosynthetic performance and long-term production phase. Furthermore, the final total Chl content of cells in the PVA-Ca<sup>2+</sup>-TCNF matrix increased *ca.* two-fold during 7 days (Fig. 6A), whereas the total Chl content of the cells in vials with destroyed Ca<sup>2+</sup>-alginate was ~2.5-times higher (Fig. 6B). This difference indicates that the growth of the cells entrapped in PVA-Ca<sup>2+</sup>-TCNF matrices is restricted as compared to the partially suspended cells in destroyed Ca<sup>2+</sup>-alginate. The growth restriction might allow the cell metabolism to shift more towards ethylene production.

At the end of the stationary phase of ethylene production (at 8 days), the photosynthetic activity of all cells had substantially decreased in all samples due to their prolonged exposure to a closed system (Fig. 6C). However, a bleaching effect was observed only in the cells in destroyed Ca<sup>2+</sup>-alginate, which is also reflected in their decreased Chl content at 8 days (Fig. 6B).

For the long-term operational capacity of the system, the cells must maintain high levels of photosynthetic activity after periodic refreshment of medium nutrients and Ci source. In our multi-cycle photosynthetic activity monitoring experiment in closed conditions and in the presence of 200 mM NaHCO<sub>3</sub>, WT cells entrapped within PVA-Ca<sup>2+</sup>-TCNF retained high photosynthetic activity after two refreshment cycles. In contrast, the operational capacity of the destroyed Ca<sup>2+</sup>-alginate was lost after the first refreshment cycle (Fig. S6†). Overall, our results indicate that the cells entrapped in PVA-Ca<sup>2+</sup>-TCNF matrices can be subjected to a long-term production phase due to high mechanical properties of the colloidal cross-linked fibril matrix, which protects the cells and enables good fitness even in submerged conditions with NaHCO<sub>3</sub> supplement.

## Conclusions

We fabricated a novel immobilization matrix design for photosynthetic cell factories with superior performance in mechanical strength, long-term cell fitness, matrix stability and ethylene productivity in challenging submerged conditions, when compared with the existing alginate-based alternatives.

The matrix utilises never-dried TCNF cross-linked with PVA and Ca<sup>2+</sup> (PVA-Ca<sup>2+</sup>-TCNF). After partial drying, PVA-Ca<sup>2+</sup>-TCNF forms self-standing hydrogel films with higher wet-strength than in Ca<sup>2+</sup>-alginate films. This is due to the colloidal nature of TCNF and their ability to form strong cross-links with PVA in contrast to the reversible ionic bonding between polymeric alginate and Ca<sup>2+</sup>. Observed *via* rheology, the critical stress of wet PVA-Ca<sup>2+</sup>-TCNF is over three times higher than in Ca<sup>2+</sup>-alginate. Moreover, cyanobacterial cells immobilised in PVA-Ca<sup>2+</sup>-TCNF maintain optimal photosynthetic activity during partial drying and demonstrate faster cell recovery from stress caused by drying. Importantly, improved photosynthetic activity of

immobilised cyanobacterial cells is also observed in PVA-Ca<sup>2+</sup>-TCNF with low initial moisture content when submerged in cultivation medium due to the mechanical stability and hygroscopicity of the TCNF network. These results may also suggest that the TCNF matrix has more favourable porosity compared to alginate and investigating this in more detail is a topic for future efforts. Finally, PVA-Ca<sup>2+</sup>-TCNF matrices remained stable under submerged cultivation for ethylene production in the presence of NaHCO<sub>3</sub> supplement with no cell leakage, while the Ca<sup>2+</sup>-alginate matrices disintegrated within 20 minutes, causing most of the cells to leak into the medium. Thus, the ethylene-producing *Synechocystis* sp. PCC 6803 cells immobilized within PVA-Ca<sup>2+</sup>-TCNF demonstrated improved photosynthetic activity with restricted growth and higher ethylene productivity throughout the experiment than the cells in the destroyed Ca<sup>2+</sup>-alginate. These results highlight the versatility and potential of this immobilization matrix design for long-term chemicals production.

## Conflicts of interest

There are no conflicts to declare.

## Acknowledgements

This research was financially supported by the NordForsk NCoE program “NordAqua” (project 82845), the Academy of Finland (AlgaLEAF, project no. 322752, 322754 and 322755). This project has received funding from the European Union’s Horizon 2020 research and innovation programme under grant agreement No 899576. The work is a part of the Academy of Finland’s Flagship Programme under Projects No. 318890 and 318891 (Competence Center for Materials Bioeconomy, FinnCERES). Dr Suvi Arola was supported by the Academy of Finland postdoctoral fellow grant no 311608 and 326262. We are thankful to Dr Valentina Guccini for help in AFM imaging.

## References

- 1 A. Hitchcock, C. N. Hunter and D. P. Canniffe, *Microbiol. Biotechnol.*, 2020, **13**, 363–367.
- 2 R. Miao, H. Xie, X. Liu, P. Lindberg and P. Lindblad, *Curr. Opin. Chem. Biol.*, 2020, **59**, 69–76.
- 3 J. Ungerer, L. Tao, M. Davis, M. Ghirardi, P. C. Maness and J. Yu, *Energy Environ. Sci.*, 2012, **5**, 8998–9006.
- 4 S. Vajravel, S. Sirin, S. Kosourov and Y. Allahverdiyeva, *Green Chem.*, 2020, **22**, 6404–6414.
- 5 M. C. Flickinger, J. L. Schottel, D. R. Bond, A. Aksan and L. E. Scriven, *Biotechnol. Prog.*, 2007, **23**, 2–17.
- 6 L. E. de-Bashan and Y. Bashan, *Bioresour. Technol.*, 2010, **101**, 1611–1627.
- 7 A. Léonard, P. Dandoy, E. Danloy, G. Leroux, C. F. Meunier, J. C. Rooke and B. L. Su, *Chem. Soc. Rev.*, 2011, **40**, 860–885.



- 8 S. Vasilieva, E. Lobakova and A. Solovchenko, in *Environmental Biotechnology* Vol. 3, Springer, Cham, 2021, pp. 193–220.
- 9 S. Kosourov, G. Murukesan, M. Seibert and Y. Allahverdiyeva, *Algal Res.*, 2017, **28**, 253–263.
- 10 S. N. Kosourov, M. He, Y. Allahverdiyeva and M. Seibert, *Microalgal hydrogen production: achievements and perspectives*, 2018, **16**, 355–383.
- 11 S. N. Kosourov and M. Seibert, *Biotechnol. Bioeng.*, 2009, **102**, 50–58.
- 12 H. Leino, S. N. Kosourov, L. Saari, K. Sivonen, A. A. Tsygankov, E. M. Aro and Y. Allahverdiyeva, *Int. J. Hydrogen Energy*, 2012, **37**, 151–161.
- 13 M. Jämsä, S. Kosourov, V. Rissanen, M. Hakalahti, J. Pere, J. A. Ketoja, T. Tammelin and Y. Allahverdiyeva, *J. Mater. Chem. A*, 2018, **6**, 5825–5835.
- 14 N. Mallick and L. C. Rai, *World J. Microbiol. Biotechnol.*, 1994, **10**, 439–443.
- 15 P. Sikareepaisan, U. Ruktanonchai and P. Supaphol, *Carbohydr. Polym.*, 2011, **83**, 1457–1469.
- 16 T. Saito, Y. Nishiyama, J. L. Putaux, M. Vignon and A. Isogai, *Biomacromolecules*, 2006, **7**, 1687–1691.
- 17 M. Hakalahti, A. Salminen, J. Seppälä, T. Tammelin and T. Hänninen, *Carbohydr. Polym.*, 2015, **126**, 78–82.
- 18 H. Dong, J. F. Snyder, K. S. Williams and J. W. Andzelm, *Biomacromolecules*, 2013, **14**, 3338–3345.
- 19 R. Pereira, A. Carvalho, D. C. Vaz, M. H. Gil, A. Mendes and P. Bártolo, *Int. J. Biol. Macromol.*, 2013, **52**, 221–230.
- 20 K. Thiel, E. Mulaku, H. Dandapani, C. Nagy, E. M. Aro and P. Kallio, *Microb. Cell Fact.*, 2018, **17**, 34.
- 21 R. Rippka, J. Deruelles and J. B. Waterbury, *Microbiology*, 1979, **111**, 1–61.
- 22 M. Hakalahti, M. Faustini, C. Boissière, E. Kontturi and T. Tammelin, *Biomacromolecules*, 2017, **18**, 2951–2958.
- 23 H. K. Lichtenthaler, *Methods Enzymol.*, 1987, **148**, 350–382.
- 24 J. L. Drury, R. G. Dennis and D. J. Mooney, *Biomaterials*, 2004, **25**, 3187–3199.
- 25 J. W. Rhim, *LWT – Food Sci. Technol.*, 2004, **37**, 323–330.
- 26 B. T. Stokke, K. I. Draget, O. Smidsrød, Y. Yuguchi, H. Urakawa and K. Kajiwara, *Macromolecules*, 2000, **33**, 1853–1863.
- 27 H. Park, S. W. Kang, B. S. Kim, D. J. Mooney and K. Y. Lee, *Macromol. Biosci.*, 2009, **9**, 895–901.
- 28 S. E. C. Whitney, M. G. E. Gothard, J. T. Mitchell and M. J. Gidley, *Plant Physiol.*, 1999, **121**, 657–663.
- 29 B. A. Harper, S. Barbut, L. T. Lim and M. F. Marcone, *J. Food Sci.*, 2014, **79**, E562–E567.
- 30 A. Walther, F. Lossada, T. Benselfelt, K. Kriechbaum, L. Berglund, O. Ikkala, T. Saito, L. Wågberg and L. Bergström, *Biomacromolecules*, 2020, **21**, 2536–2540.
- 31 M. Hakalahti, A. Mautner, L. S. Johansson, T. Hänninen, H. Setälä, E. Kontturi, A. Bismarck and T. Tammelin, *ACS Appl. Mater. Interfaces*, 2016, **8**, 2923–2927.

